Laser-Layered Microfabrication of Spatially Patterned Functionalized Tissue-Engineering Scaffolds

Gazell Mapili,[1] Yi Lu,[2] Shaochen Chen,[2] Krishnendu Roy[1]

[1] Department of Biomedical Engineering, The University of Texas at Austin, Austin, Texas 78712

[2] Department of Mechanical Engineering, The University of Texas at Austin, Austin, Texas 78712

Received 22 December 2004; revised 9 February 2005; accepted 23 February 2005
Published online 15 July 2005 in Wiley InterScience (www.interscience.wiley.com). DOI: 10.1002/jbm.b.30325

Abstract: Understanding cell behavior inside complex, three-dimensional (3D) microenvironments with controlled spatiotemporal patterning of physical and biochemical factors would provide significant insights into the basic biology of organ development and tissue functions. One of the fundamental limitations in studying such behavior has been the inability to create patterned microenvironments within 3D scaffold structures. Here a simple, layer-by-layer stereolithography (SL) method that can precisely pattern ligands, extracellular-matrix (ECM) components, and growth factors, as well as controlled release particles inside a single scaffold, has been developed. The process also allows fabrication of predesigned internal architectures and porosities. Photocrosslinkable poly(ethylene glycol) dimethacrylate (PEGDMA) was used as the basic structural component of these microfabricated scaffolds. PEG acrylates, covalently modified with the cell adhesive peptide arginine-glycine-aspartic acid (RGD) or the ECM component heparan sulfate, was incorporated within the scaffolds to facilitate cell attachment and to allow spatial sequestration of heparan-binding growth factors. Fluorescently labeled polymer microparticles and basic fibroblast growth factor (FGF-2) were chosen to illustrate the capability of SL to spatiotemporally pattern scaffolds. The results demonstrate that a precise, predesigned distribution of single or multiple factors within a single 3D structure can be created, and specific internal architectures can be fabricated. Functionalization of these scaffolds with RGD is demonstrated, and heparan sulfate allows efficient cell attachment and spatial localization of growth factors. Such patterned scaffolds might provide effective systems to study cell behavior in complex microenvironments and could eventually lead to engineering of complex, hybrid tissue structures through predesigned, multilineage differentiation of a single stem-cell population. © 2005 Wiley Periodicals, Inc. J Biomed Mater Res Part B: Appl Biomater 75B: 414–424, 2005

Keywords: scaffolds; tissue engineering; 3D micropatterning; stem cells; stereolithography; microfabrication

INTRODUCTION

In recent years significant milestones have been achieved in the field of tissue engineering. One of the fundamental limitations in current efforts, however, has been the inability to produce multiple tissue types (e.g., bone, cartilage, ligaments, muscles, etc.) in a predesigned fashion inside a single scaffold structure.[1,2] Although stem cells have been shown to differentiate into a variety of cell types, simultaneous construction of hybrid tissue structures within a single three-dimensional (3D) environment resembling the complex architecture of organs are yet to be reported. The basic barrier in creating such structures is a lack of knowledge on how stem cells behave and differentiate under spatiotemporally distributed biochemical and physical microenvironments, similar to those encountered during organ development.

Most patterning techniques to study cell behavior have been developed for two-dimensional (2D) surfaces.[3–5] Although these studies have provided tremendous insights into a variety of cellular processes and interactions, cell behavior within controlled 3D microenvironments have not been studied. Currently, most 3D scaffolding techniques only allow us to incorporate biofactors in bulk, that is, the factors are distributed randomly throughout the matrix. Even recent attempts in free-form fabricated scaffolds[6–9] or scaffolds with multiple sustained released factors[10] have only reported bulk incorporation. Complex spatial patterning along with temporal distribution of signaling molecules in the immediate mi-

Correspondence to: Krishnendu Roy (e-mail: kroy@mail.texas.edu)
Contract grant sponsor: The Whitaker Foundation
Contract grant sponsor: National Science Foundation; contract grant numbers: BES-0313425, DMI-222014

croenvironment of stem cells, a hallmark of native tissue development, has yet to be engineered and studied.

The two fundamental steps toward achieving patterned microenvironments inside scaffold structures are (a) creating localized concentrations (or gradients) of multiple growth factors by controlled spatial incorporation while preventing their diffusion to surrounding areas and (b) creating a temporal gradient of growth factors, that is, being able to precisely deliver several growth factors in a physiologically relevant time sequence. This article presents efforts to achieve micropatterned scaffold structures by a layer-by-layer microfabrication approach, with photopolymerizable poly(ethylene glycol) (PEG) -based hydrogels and polymer microparticles. The goal is to create precise, predesigned spatial distribution of multiple entities inside a single scaffold and to mimic the physiological environment from which a single progenitor population can differentiate into multiple tissue lineages.

A laser-based, layer-by-layer, stereolithography approach for photocrosslinking biofunctionalized, acrylated PEG monomers carrying soluble and entrapped particles to achieve spatial patterning has been developed. Photocrosslinked hydrogel-based scaffolds, both degradable and non-degradable, have been widely investigated for musculoskeletal tissue engineering. Several researchers have demonstrated that PEG-based hydrogels can be successfully used to culture chondrocytes and osteocytes for bone- and cartilage-specific tissue regeneration.[6,11–15] Others have developed hydrogels (using synthetic or natural polymers) having specific functionalities and degradation characteristics for a similar purpose.[16–18] Osteogenic differentiation of mesenchymal stem cells (MSCs) within PEG-based hydrogels has also been demonstrated by Nuttelman et al.[19] and Anseth et al.[20] However, most of these approaches use bulk encapsulation of cells and factors to create either bone or cartilage. Recent efforts to create hybrid structures have been reported with the use of *in vitro* derived osteocytes and chondrocytes (from MSCs) followed by incorporation of those precursor cells in different layers prior to *in vivo* implantation.[21,22] Attempts to direct a single stem cell population into multiple lineages within a single scaffold structure by creating patterned growth factor distribution have not yet been reported. In addition, PEG-based scaffolds with designed internal structures and porosities for cell seeding and subsequent study of progenitor cells in complex microenvironments are yet to be demonstrated.

A key concept in creating localized patterning of biofactors is the ability to prevent or control their diffusion into surrounding areas. In native tissue such spatial patterning is created by various extracellular matrix (ECM) components that bind to and sequester specific growth factors. It was hypothesized that functionalizing the patterned scaffolds with ECM components (e.g., heparan sulfate) would allow the entrapped growth factors in specific regions to be sequestered, thereby maintaining the spatial patterning. Components of the ECM not only play a significant role in cell adhesion and migration but also support optimal cell differentiation through molecular signaling by creating local concentration gradients of growth factors (reviewed by Taipale and Keski-Oja[23]). Orban, Marra, and Hollinger[2] discussed the need for tissue-engineering scaffolds to incorporate factor-immobilization concepts, because local concentrations of growth factors play a key role in directing lineage-specific differentiation of progenitor cells. Highly charged glycosoaminoglycans (GAG), for example, heparan sulfates in the ECM, bind to soluble signaling molecules, thereby preventing diffusion and creating local concentrations and optimal signaling, especially for basic fibroblast growth factor, FGF-2.[24–30] Here it is shown that heparan incorporation into PEG scaffolds can create localized concentrations of growth factors, thereby producing predesigned spatial patterning.

It is further demonstrated that polymer microparticles can be spatially incorporated within the scaffolds, thereby providing evidence that eventually controlled-release carriers with various release kinetics can be used to create temporal patterns along with spatial distributions. Murine marrow stromal cells were successfully incorporated within these patterned structures by direct seeding on arginine-glycine-aspartic acid (RGD)-functionalized scaffolds. For the short term, such predesigned structures could be a valuable tool to study stem-cell differentiation in complex microenvironments and might eventually enable complex tissue structures to be fabricated from a single progenitor population.

MATERIALS AND METHODS

PEGDMA Solutions and Photoinitiators

Poly(ethylene glycol) dimethacrylate (PEGDMA, $n = 1000$, Polysciences, Inc.), was dissolved in phosphate-buffered saline (PBS) to form either 10–20% (w/v) or 100% (w/v) solutions. The photoinitiator, 2-hydroxy-1-[4(hydroxyethoxy)phenyl]-2-methyl-1-propanone (Irgacure 2959, Ciba Geigy), was used to generate free radicals for the induction of chain polymerization, with a concentration of 0.05 wt % for the lower-concentration PEGDMA solutions (10–20% w/v) or 0.07 wt % for the 100% (w/v) PEG solution. The photoinitiator was first dissolved in PBS at a maximum concentration of 0.7 wt % to ensure complete solubility, and subsequently added to the PEGDMA solutions.[31] Prepared macromer solutions were kept in a dark environment to inhibit the precrosslinking of the polymer by incidental exposure to ambient light.

Pretreatment of Glass Coverslips

Surfaces of glass coverslips were modified with an organosilane to covalently bond the hydrogel upon polymerization, thereby promoting a strong adhesion with the hydrogels when rinsed with PBS or placed in buffered solutions/cell medium.[32] Surface-tethered methacrylate groups, which covalently attach to the acrylate groups of PEGDMA upon photopolymerization, were created on the surface of glass coverslips by first immersing the slides in a solution of 3:1 ratio of 30% (w/v) H_2O_2 in distilled water and H_2SO_4. The

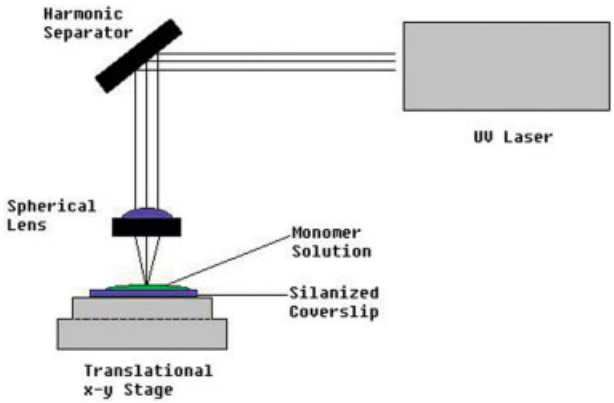

Figure 1. Experimental setup of the laser-based layer-by-layer stereolithography process for fabrication of patterned scaffolds. [Color figure can be viewed in the online issue, which is available at www.interscience.wiley.com.]

hydroxylated slides were then immersed in 1 m*M* solution of 3-(trichlorosily)propyl methacrylate in a 4:1 solution of heptane and carbon tetrachloride. All chemicals were purchased from Sigma-Aldrich, unless otherwise noted.

Microfabrication of PEG Scaffolds with a Frequency-Tripled Nd:YAG Laser

With the use of a 100% (w/v) PEGDMA solution with photoinitiator, 3D scaffolds were fabricated in an experimental setup with the third harmonic wave of an Nd:YAG laser (λ = 355 nm, *Surelite* from Continuum, Figure 1), which generated nanosecond pulses. The laser energy was measured to be ~10 mJ/pulse. Macromer solutions were placed on a manually operated 3D micromanipulator stage. The stage carrying the liquid macromer solutions was translated in the *x-y* direction at a scanning speed of approximately 50 μm/s in order to create predesigned patterns within a single layer of a tissue-engineering scaffold. The unpolymerized solution was washed off with PBS. This process is repeated for each different macromer solution composition to create single- or multilayered patterned scaffolds.

Fluorescently labeled latex microparticles (5.47 μm Cy5, 0.93 μm FITC, and 1.0 μm TRITC, Bangs Laboratories, Inc.) were added to the macromer solutions at varying concentrations (ranging from 1% to 10% v/v) prior to crosslinking in order to show the capabilities of this laser setup not only to encapsulate the particles during polymer crosslinking, but to pattern them in a predesigned fashion. Vertical patterning, that is, in the *z* direction, was achieved by creating two-layered scaffolds. Macromer solution containing Cy5-labeled particles was selectively polymerized in a grid-type geometry. The unpolymerized solution was washed off extensively, and a second macromer solution containing FITC-labeled particles was polymerized over the first layer in the same geometry. These constructs were analyzed with the use of either a confocal microscope (Leica SP2 AOBS), or scanning electron microscopy (Phillips 515 SEM). Z slices obtained by confocal fluorescence microscopy were reconstructed to create 3D images of the entire scaffolds.

RGD and Heparan Conjugation to PEG

Figure 2 shows the reaction scheme for functionalizing the scaffold material. A well-characterized fibronectin-derived peptide, YRGDS (tyrosine-arginine-glycine-aspartic acid-serine, Bachem Biosciences Inc., Torrance, CA), was reacted in equimolar amounts with acryloyl-PEG-*N*-hydroxysuccin-

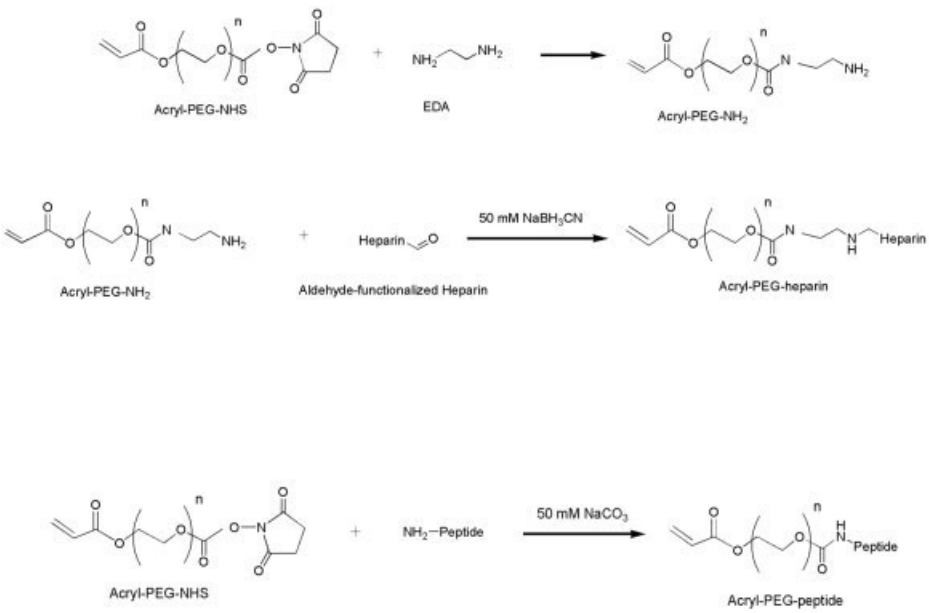

Figure 2. Reaction schemes detailing the conjugation of heparan and RGD to acrylated polyethylene glycols.

imide (acryl-PEG-NHS, M_w 3400, Nektar Therapeutics Inc.).[14,18] Sodium bicarbonate buffer (pH 8.2) (200 μL) was added to acryl-PEG-NHS, which, in a drop-wise fashion, was added to the YRGDS solution (1 mg/mL in sodium bicarbonate buffer). Conjugation was completed in a dark environment for 3 h at room temperature. Peptide-modified PEG-acryl was frozen in liquid nitrogen, lyophilized for 24 h, and stored in a dessicator at −20°C until further use.

To create a heparan moiety onto PEG acrylates, ethylenediamine (EDA) was first reacted in excess with acryl-PEG-NHS at a 5:1 molar ratio to yield acryl-PEG-NH_2, similar to the method for RGD conjugation. The reaction was completed for 3 h at room temperature in a dark environment followed by extensive dialysis (Tube-o-dialyzer, MWCO 1000, Geno Technologies, St. Louis, MO) of unreacted EDA. Samples were frozen and lyophilized for 24 h. Periodated heparan (Celsus Laboratories Inc.) was reacted in equimolar amounts for 3 h in a dark environment with acryl-PEG-NH_2 to yield acryl-PEG-heparan in the presence of 50 m*M* $NaBH_3CN$ as the reducing agent. Heparan, containing aldehyde moieties, undergoes Schiff-base reactions with organic amines, and if treated with $NaBH_3CN$, the Schiff-base intermediate is reduced to its corresponding amine, forming an irreversible bond. Dialysis (Tube-o-dialyzer, MWCO 1000, Geno Technologies, St. Louis, MO) was performed to eliminate the reducing agent, and the product was lyophilized and stored in a dessicator at −20°C until further use.

Cell Culture

Murine OP-9 marrow stromal cells (a gift from T. Reid, University of Toronto) were cultured in Minimum Essential Medium-Alpha (Gibco Invitrogen Corp.) supplemented with 20% fetal bovine serum, 30 m*M* sodium bicarbonate (Sigma-Aldrich Co.), 2 m*M* L-glutamine (Gibco Invitrogen Corp.), 50 μg/mL penicillin–streptomycin (Gibco Invitrogen Corp.), and 100 m*M* of β-mercaptoethanol (Sigma-Aldrich Co.). Cells were passaged every 2–3 days.

An amine-reactive fluorescent dye, CellTrace™ Far Red DDAO-SE (Molecular Probes, Eugene, OR) was used as a cell tracer to study cell attachment onto RGD-modified scaffolds. The succinimidyl ester reactive group of the dye forms a covalent attachment to primary amines that occur in proteins and other biomolecules on the inside and outside of cells. Because the fluorescent tag is inherited by daughter cells even after multiple divisions, cells were labeled in culture before their use in cell-attachment studies. Additionally DAPI (Molecular Probes, Eugene OR) was also used to stain for cell nuclei. All cell staining were performed according to manufacturer's protocol.

Cell Attachment to RGD-Modified Hydrogels

Acryl-PEG-RGD at a concentration of 5.0 m*M* was added to a 100% (w/v) PEGDMA solution with I2959 as the photoinitiator. Single-layered scaffolds ($2 \times 2 \times 0.5$ mm^3, $L \times W \times H$) with defined porosities were fabricated. The scaffolds were UV sterilized overnight in a cell-culture hood prior to cell seeding. Parafilm was placed in a nontreated cell-culture plate in order to form a hydrophobic surface when seeding the cells, and the scaffolds were placed on top of the film. Fluorescently labeled murine bone-marrow stromal cells (OP-9) were seeded on both the unmodified and RGD-modified constructs at a density of 2×10^4/scaffold using 200 μL of medium. Medium was added to the culture plate after a 4-h seeding period. The scaffold-cell constructs were cultured for 24 h, and then rinsed with prewarmed PBS to remove nonimmobilized cells. Cells were fixed onto the scaffolds using 4% paraformaldeyde (pH 7.3) solution for 4 h at 37°C. DAPI was used to stain for cell nuclei upon fixation. The scaffolds were imaged with confocal fluorescence microscopy and critical-point dried for SEM (Phillips 515) analysis.

FGF-2 Binding to Heparan-Modified PEG

On separate methacrylate-treated coverslips, thin-layered hydrogels were fabricated with the use of 10% (w/v) PEGDMA with photoinitiator and 10% acryl-PEG-heparan. Each thin-layered hydrogel encapsulated 2 μg of FGF-2 (R&D Systems). Unbound FGF-2 was allowed to diffuse out of the hydrogels overnight while incubating in PBS at 37°C. The PBS solution in which the substrates were submersed was replaced three times during a 24-h period of incubation to remove released FGF-2. To evaluate for FGF-2 binding to heparan-modified hydrogels, immunostaining was performed with the use of primary anti-FGF antibody, biotinylated-secondary antibody, and streptavidin-FITC. The binding times for the antibodies and streptavidin-FITC were 1 h each. Fluorescence microscopy was used to detect FGF-2 immobilization within the hydrogels.

To test for FGF-2 binding in the multilayered models, a two-layered hydrogel construct was polymerized with the use of a UV lamp (365 nm, intensity ~4 mW/cm^2) and a $3 \times 3 \times 1$ mm^3 plastic molding. The first layer, with 20% (w/v) PEGDMA and 0.05 wt% I2959 solution, was partially polymerized by exposure to the UV light for 4 min. The second macromer solution, which had 5.0 m*M* acryloyl-PEG-heparan and 2 μg of FGF-2 in addition to the 20% PEGDMA solution, was polymerized over the first layer by exposure to UV light for 10 min. The hydrogel construct was then placed in PBS buffer (pH 7.4) for a period of 3 days. The construct was transversely sliced, and immunostaining was completed, as described previously, to evaluate for FGF-2 binding.

RESULTS

Microfabrication of Single- and Multilayered Scaffolds with Precise Internal Features

The laser-based stereolithography method was used to create polymer scaffold structures with specific pore/channel dimensions. FITC-labeled latex microparticles were incorporated into the macromer solution prior to laser exposure in order to

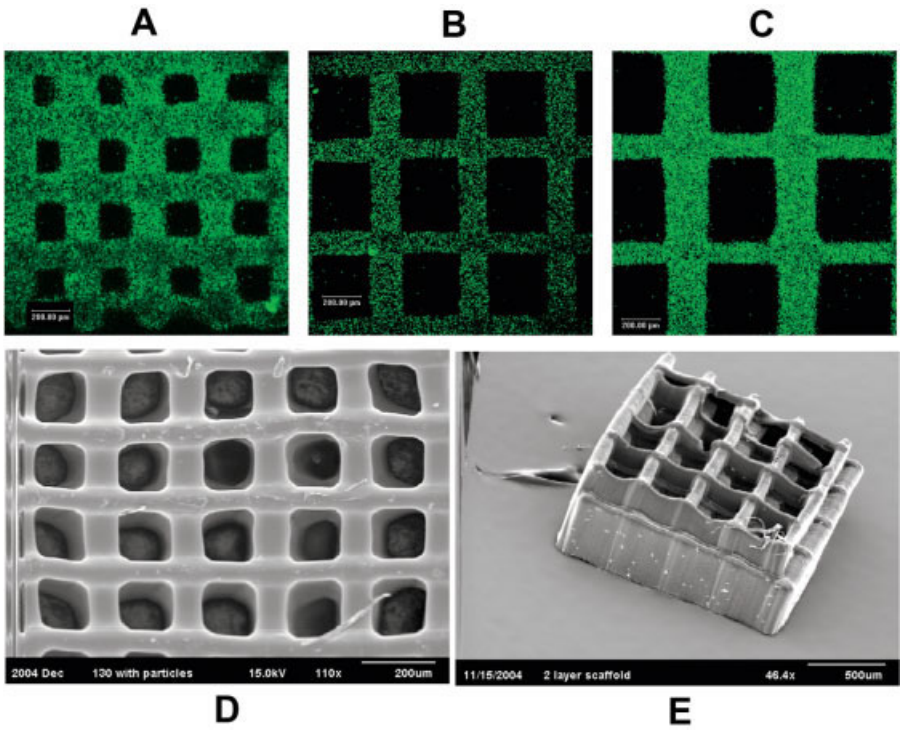

Figure 3. Confocal microscope images and SEM micrographs show scaffolds with precise internal geometries can be fabricated with the use of the stereolithography method. (A)–(C) Confocal microscopic images showing scaffolds formulated with 100% (w/v) PEGDMA, 0.07 wt % Igracure 2959, and 1% (w/w) FITC-labeled latex particles. Size bar shown is equal to 200 μm. Scaffold dimensions for each scaffold (A–C) are listed in Table I. SEM micrographs in (D) and (E), formulated in the same concentrations of PEGDMA and I2959, represent a single-layer scaffold and a multilayered scaffold, respectively. In order to differentiate the layers within a single scaffold during SEM analysis, the first layer of (E) was polymerized to have a thicker wall dimension then the second layer. [Color figure can be viewed in the online issue, which is available at www.interscience.wiley.com.]

demonstrate the ability to incorporate controlled-release carriers or biomolecules within the scaffold, as well as for easy visualization using confocal fluorescence microscopy. Porous scaffolds were fabricated with line spacings (center to center) of 300, 400, and 500 μm, respectively. As shown in Figure 3(A–C), precise and highly controlled internal architectures can be generated during scaffold fabrication. Pores (channels) of sizes ~175, 300, and 350–400 μm were achieved with the use of the indicated line spacing within a single 3D scaffold layer. As evident, highly uniform pore distribution was achieved with the use of this technique. Table I shows the detailed geometrical characterization of the scaffolds. The data also demonstrate that biofactors and microparticles can be easily incorporated within the scaffold walls during the fabrication process. It is to be noted that the horizontal walls are slightly narrower than the vertical ones. This is because the *x*-direction movement of the stage is computer controlled at 50 μm/s, whereas the movement in the *y* direction is manually controlled to achieve an equivalent speed. Minor discrepancies in laser scanning speed could create such differences in wall thickness (a slower speed results in a thicker polymerized area).

Figure 3(D) shows a scanning electron micrograph of a representative, single-layer scaffold, whereas Figure 3(E) demonstrates the ability to create multiple layers. The two-layer scaffold shown in Figure 3(E) also provides evidence that layers with various wall thickness and dimensions can be created by this approach.

TABLE I. Geometric Characteristics of the Microfabricated Scaffolds Shown in Figure 3(a–c)

	Distance Between Center of Lines			
	Theoretical	Measured	Measured Pore Size	Measured Wall Thickness
Scaffold A	300 μm	~350μm	~175μm×175μm	~140μm,200μm
Scaffold B	400 μm	~450μm	~300μm×350μm	~90μm,120μm
Scaffold C	500 μm	~565μm	~350μm×425μm	~100μm,200μm

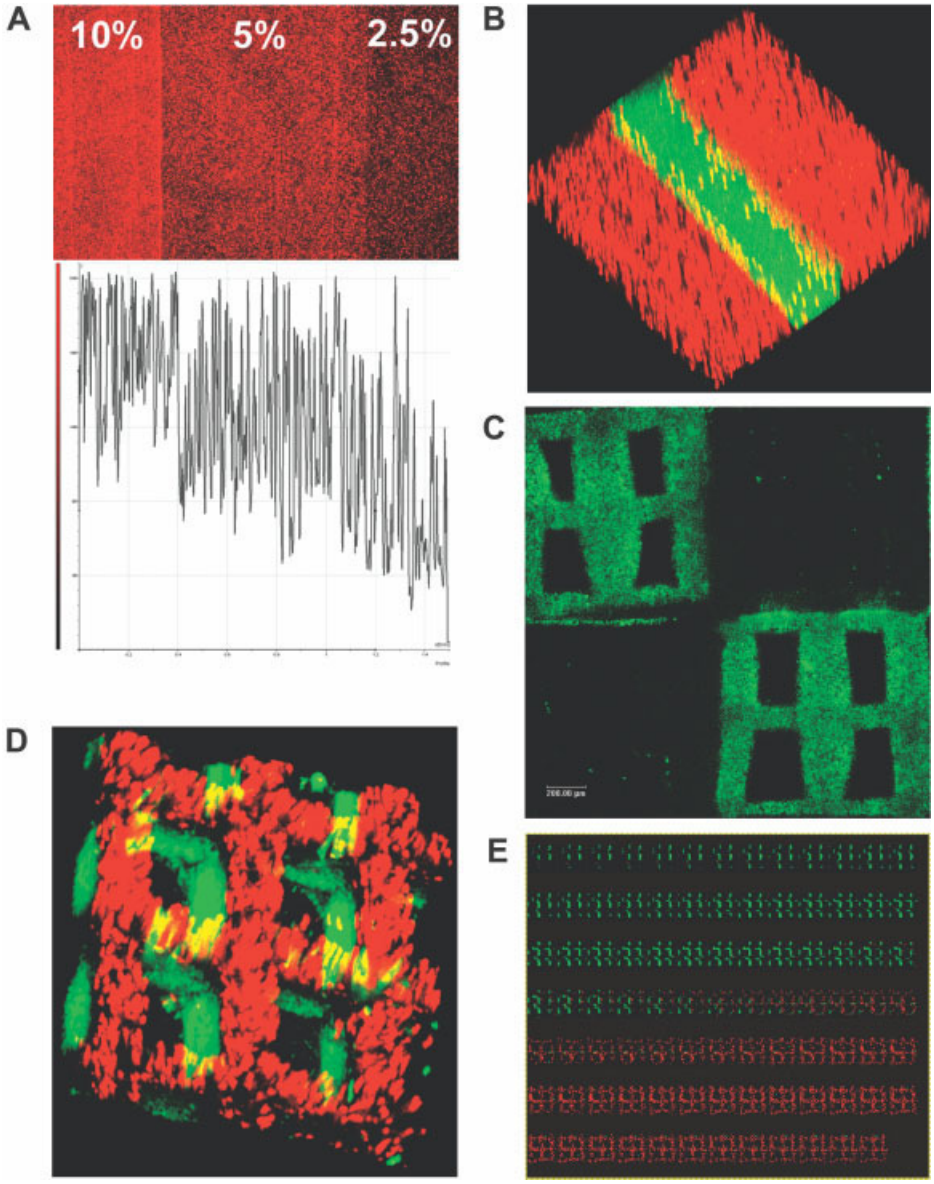

Figure 4. Laser-based SL can create predesigned, spatially patterned scaffold structures. Scaffolds shown here are formulated with 100% (w/v) PEGDMA and 0.07 wt % I2959. (A) Decreasing amounts of TRITC-labeled latex particles that are linearly patterned in a gradient form. The concentrations from left to right are 10%, 5%, and 2.5% (w/w) of particles in macromer solution. The graph below shows the intensity profile indicating decreasing fluorescence (and hence particle concentration) from left to right. (B) and (C) Spatial patterning with either FITC- or Cy5-labeled latex particles, as well as the capability of the laser SL to create uniform, precise channels (pores) within a scaffold. (D) A 3D reconstruction of a multilayered scaffold with confocal z slices. The individual slices through the scaffold are shown in (E) as a composite picture. The channel porosity within this particular multilayered scaffold was measured to be approximately 400 μm.

Predesigned Spatial Patterning of Scaffold Structures Can Be Achieved with Laser Fabrication

A key feature of this stereolithography method for scaffold fabrication is its ability to create predesigned spatial patterns of single or multiple molecules and particles. The ability and flexibility of this technique has been demonstrated with the use of both single-layer (2D) and multilayer (3D) structures as well as in structures with precise internal architectures. As shown in Figure 4(A), TRITC-labeled latex particles can be spatially patterned within a single polymer layer in a decreasing particle concentration (10%, 5%, and 2.5% w/w). The line graph indicates the fluorescence intensity (and hence a measure of particle concentration) across the polymer layer and demonstrates the feasibility of creating gradients of single growth factors as well as controlled-release particles within the scaffold. Figure 4(B) demonstrates patterning of multiple agents in a single layer. Cy5 or FITC-labeled particles were incorporated in the macromer

solutions prior to laser exposure. Each pattern (line) was written with the laser, and the unpolymerized polymer-particle solution was washed off prior to polymerization of the second line using a different polymer-particle solution. This shows the ability of this fabrication process to create precise and predetermined distribution of multiple factors.

Figure 4(C) provides evidence on the feasibility of combining internal porosities and architectures along with spatial patterning inside a scaffold. A scaffold was fabricated with the use of FITC-labeled particle-carrying polymer as well as polymer without the presence of any other agents. As shown, a predesigned quadrant pattern was created with the use of the stereolithography method in which the particles were specifically sequestered in quadrants 1 and 4, whereas no factors were incorporated in quadrants 2 and 3. In addition, channels of dimension 100 μm were created during the fabrication process.

Figure 4(D,E) demonstrates the ability of this process to create multilayered, 3D structures with spatially distributed factors. Either Cy5 or FITC-labeled polymer microparticles were incorporated within each layer during photopolymerization with the laser while creating uniform pores of dimension 400 μm. Figure 4(D) shows a stacked-confocal picture (3D reconstruction) whereas Figure 4(E) is a collage of confocal slices through vertical sections of the scaffold. This suggests that both lateral (C) and vertical (D,E) patterning and can be achieved with the use of this method of scaffold fabrication.

Heparan Functionalization Allows Effective Sequestration of FGF-2

In order to maintain spatial patterning of soluble growth factors inside a scaffold structure, it is critical to sequester the factors in their intended regions and control the diffusion of the growth factors within and across the spatial region. ECM components are known to participate in sequestration and localization of certain growth factors. Here it is demonstrated that covalent conjugation of heparan to PEGDMA prior to scaffold fabrication provides efficient binding of basic fibroblast growth factor (FGF-2) and localization in both single and multilayered scaffold models. In the single-layered model [Figure 5(A–D)], polymer layers containing heparan-modified PEGDMA showed efficient FGF-2 binding and sequestration as demonstrated by immunofluorescence assays 72 h after the addition of FGF-2. Matrices without heparan did not show FGF-2 immobilization. FGF-2 binding and localization was also illustrated in multilayered hydrogels [Figure 5(F)]. By observing immunostained hydrogels through confocal fluorescence microscopy, FGF-2 diffusion from the heparan-modified layer to the unmodified layer was not observed after a 72-h incubation period in aqueous medium. These findings indicate that FGF-2 specifically binds to regions of PEG scaffolds that have been covalently modified with heparan. Such functionalization concepts could provide effective means to maintain the spatial patterns created with the use of the stereolithography method and allow one to control the rate of growth factor release from the scaffold walls.

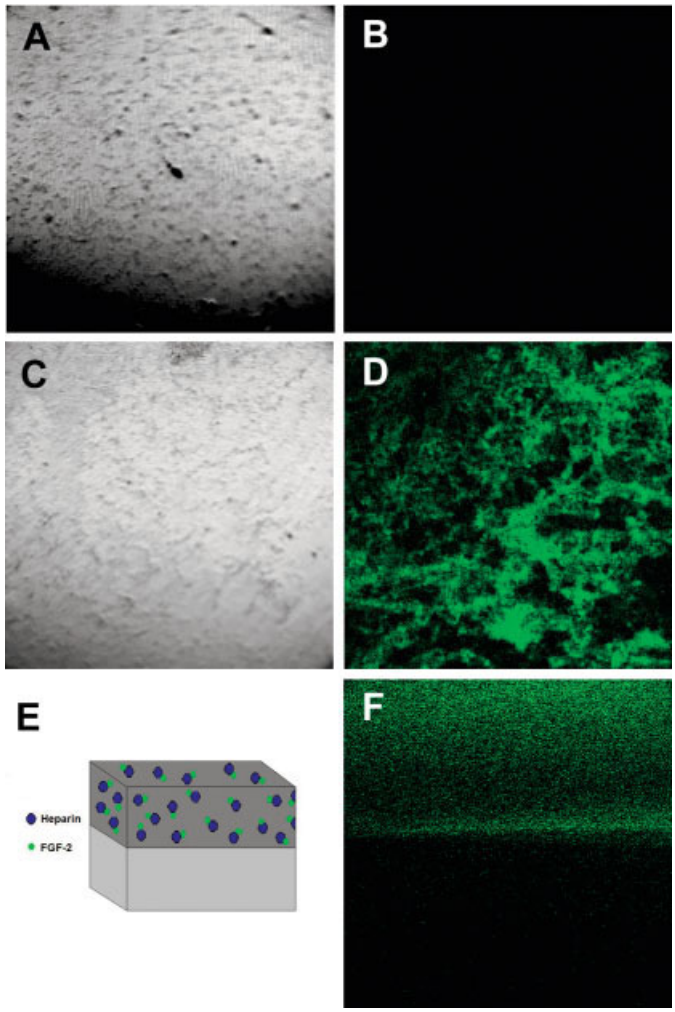

Figure 5. Incorporation of heparan in the scaffold material allows efficient FGF-2 sequestration. This was demonstrated with the use of both thin-layered polymer matrices [(A)–(D)] as well as multilayered scaffolds [(E) and (F)]. Localization of FGF-2 was evaluated by staining with biotinylated secondary antibody against FGF-2 followed by streptavidin-FITC and observing through a confocal fluorescence microscope (10× original objective). Two micrograms of FGF-2 was encapsulated in the thin-layered hydrogels and then analyzed through immunohistochemistry. Brightfield images [(A) and (C)] and fluorescence images [(B) and (D)] were captured to determine FGF-2 immobilization. Hydrogels without acryl-PEG-heparan [(A) and (B)] do not show FGF-2 binding, whereas the hydrogels that are modified with 10% acryl-PEG-heparan [(C) and (D)] show the sequestration of FGF-2. (E) A schematic of the multilayered scaffold depicted in (F). Both layers were constructed with the use of 20% (w/v) PEGDMA, 0.05% Irgacure 2959, and UV light. The top layer contains 5.0 m*M* of acryl-PEG-heparan and encapsulates 2 μg of FGF-2. (F) illustrates that FGF-2 is effectively localized only within the layer that contains heparan. [Color figure can be viewed in the online issue, which is available at www.interscience.wiley.com.]

Laser-microfabricated Scaffolds are Conducive of Cell Attachment when Functionalized with RGD

PEGDMA scaffolds containing 5 m*M* RGD-modified PEG resulted in efficient attachment and spreading of OP-9 stro-

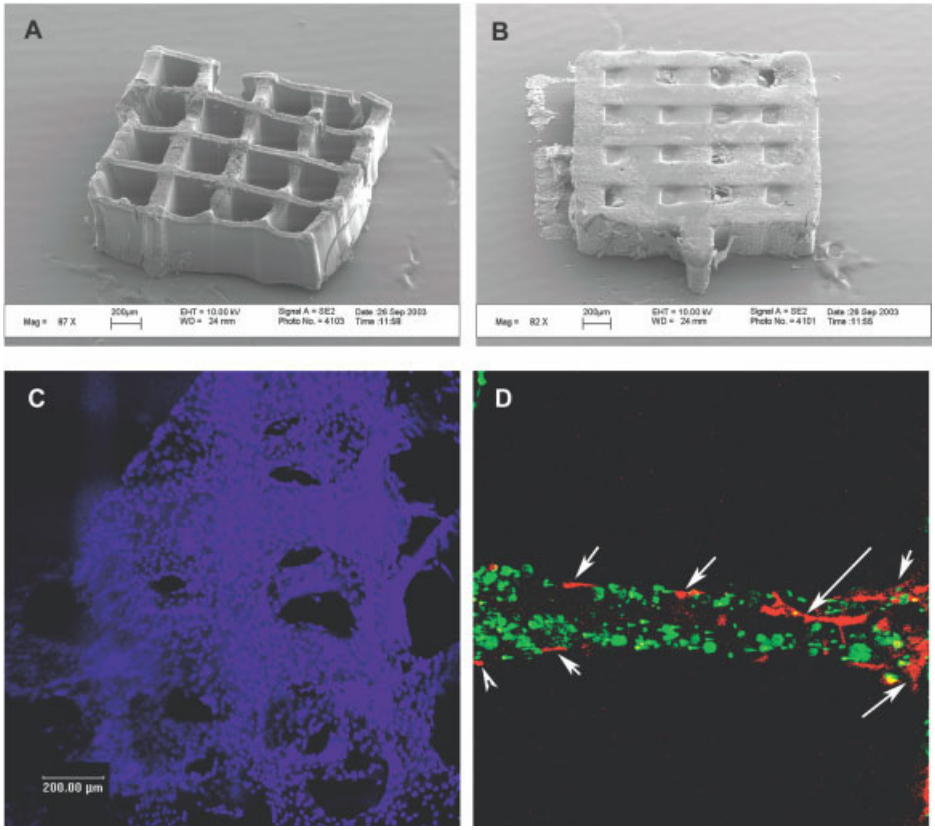

Figure 6. Incorporation of RGD in the scaffold material allows efficient cell attachment and spreading. SEM micrographs show top views of (A) a 2 × 2-mm scaffold without RGD-modification (wall thickness is ~100 μm), and of (B) a 2 × 2-mm scaffold containing 5.0 m*M* RGD-PEG-acryl (wall thickness ~200 μm). It appears that the attached OP-9 cells in (B) have secreted ECM-like materials on the scaffold. (C) and (D) Confocal fluorescence microscopy indicated that cells only attached to RGD-functionalized scaffolds. (C) DAPI nuclei staining, and (D) cells prestained with CellTracer™. The green staining seen in (D) is fluorescence from FITC-labeled particles that were encapsulated during photopolymerization.

mal cells, whereas scaffolds without the cell-adhesion peptide did not show any cell attachment. Figure 6(A,B) shows scanning electron micrographs of RGD-functionalized (B) and nonfunctionalized laser-microfabricated scaffolds that were seeded with OP-9 cells. After 24 h, no cell attachment was seen in the PEGDMA scaffolds whereas the RGD-containing scaffolds were filled with what appears to be ECM-like substances. Cell attachment on similar scaffolds was confirmed with the use of confocal fluorescence microscopy. Figure 6(C) shows DAPI staining on cells seeded on RGD-functionalized microfabricated scaffolds. It is evident that a large number of cells are attached to the scaffold walls. Figure 6(D) demonstrates cell seeding on a porous scaffold carrying FITC-labeled polymer particles. These cells were prelabeled with CellTrace™. Red fluorescence specifies the attachment of cells to the surfaces of the scaffold, and the green fluorescence indicates that entrapped polymer. The data show cells attach and spread efficiently on the scaffold wall.

DISCUSSION

One of the fundamental limitations of current efforts in the field of tissue engineering has been the inability to produce multiple tissue types in a predesigned fashion within a single construct. Recent and past methods in fabricating tissue-engineering scaffolds have only incorporated a random, bulk distribution of biofactors that are conducive to the differentiation of a single tissue type inside a 3D structure. Because complex, patterned microenvironments are necessary to develop multiple cell types within a single scaffold, spatial distribution of biofactors, as well as their temporal release kinetics, must be integrated to closely mimic the physiological environment. Furthermore, simple, easy-to-fabricate 3D scaffolds that allow the study of cells within highly controlled geometrical features as well as within predesigned patterns of biochemical and physical factors, could provide significant insights into complex cellular processes.

A laser-based SL system that can build complex scaffold structures has been developed with the use of a layer-by-layer photopolymerization process. PEGDMA was used as a model polymer because of its easy availability as well as the ability to conjugate ECM components to the polymer using well-defined chemistry. However, any polymer or resins that undergo photoinitiated free-radical polymerization can be used as long as they are cytocompatible. In addition, degradable scaffolds can also

be fabricated with the use of this process by the introduction of hydrolytically or enzymatically degradable segments within the photopolymer as described by Anseth and colleagues[13,33,34] and Halstenberg et al.[18]

The point-by-point polymerization process is similar to a raster scanning device that could eventually be completely automated. Such automated stereolithography systems are commercially available and can be computer guided. However, it must be noted that the resolution of most commercial stereolithography system remains approximately 200–250 μm. Although some commercial systems have a theoretical feature size of 75 μm, they failed to create open pores and channels when provided with a scaffold design, similar to those presented here (data not shown). Eventually such a fabrication system can be coupled to computer-aided design and manufacturing (CAD/CAM)-driven automation, and can use CT or MRI-based data as the input for designing complex scaffolds. Such systems have been described by Hollister and coworkers,[6,35–37] albeit at much larger feature sizes. The attraction of a simple laser-based system is that it can be a benchtop, research-scale system with high resolution. Although a UV laser was used because of existing data showing cytocompatibility of the photoinitiator,[13] it is conceivable that other lasers can be substituted as long as a corresponding cell-compatible photoinitiator is available.

The crosslinking of the macromer solution induced by the focused UV pulsed laser ($\lambda = 355$ nm), and the complexity of the scaffold's architecture is controlled by the translational motion of the stage in the *x-y* directions, as well as feature resolution. The laser beam can be modeled as a Gaussian distribution in which the beam's diameter at the focal waist governs the theoretical *x-y* resolution of the system, which in turn dictates the smallest feature sizes attainable (e.g., porosities or wall thickness of the scaffold). The focal waist of a Gaussian beam with a circular cross section is given by

$$w_o = (2\lambda/\pi) \times f^{\#}, \tag{1}$$

where w_0 is the laser beam radius at the focal waist, λ is the wavelength, $f^{\#}$ (f number) is given by

$$f^{\#} = f/2w_1$$

where f is the focal length of the lens, and w_1 is the beam radius at the lens. With the use of this equation, in this case, the theoretical resolution is calculated to be 5.8 μm ($\lambda = 355$ nm, $f = 25.4$ mm, and beam $w_1 = 1$ mm). Similarly, the depth-of-focus equation for a Gaussian beam with a circular cross section provides the theoretical resolution in the z axis, which in turn dictates the thickness of each layer. This can be solved by

$$\text{dof} = (\pi w_o^2/\lambda)*(\zeta^2 - 1)^{1/2}, \tag{2}$$

where dof is the depth of focus, and ζ is the acceptable focus within 2% or 1.02. For the current setup the theoretical depth of focus calculated from Eq. (2) is 15 μm. These values demonstrate that the laser-based system has the potential to be a high-resolution instrument. However, the experimental *x–y* resolution as well the z resolution of the system was measured to be $\sim$100 μm, which was governed by the amount of macromer solution placed on the translational stage. These significant deviations between the theoretical and experimental values can be caused by laser diffraction, heat conduction, photoinitiator diffusion, and scattering due to polymer particles. It is believed that through careful selection of photoinitiator, particle concentration, and optimal laser optics, this resolution can be significantly improved. However, even at its current resolution, the feature sizes of the setup are conducive of studying cell differentiation and tissue formation in a highly controlled, predesigned manner. An ideal wall thickness of a scaffold should be sufficient enough to not only encapsulate 5–10-μm-sized controlled-release particles and other biomolecules, but should provide enough surface area for stem cells to attach and spread for optimal cell-to-cell communication and differentiation. The scaffold-fabrication system developed here allows study of the effects of channel wall thickness, pore size, and polymer crosslink density (all leading to the issues of nutrient diffusivity) in a controlled and detailed manner.

The laser-layered stereolithography process has the capability of spatially patterning growth factors and ECM components by their addition into the macromer solution prior to photopolymerization. Instead of bulk photocrosslinking PEG, as reported by other groups,[11,13] laser SL provides a controlled point-by-point polymerization method of creating a predesigned scaffold. This unique capability specific to SL enables multiple types of growth factors to be spatially patterned within a single structure, overcoming a major roadblock in current efforts with creating more complex tissue-like structures. Another advantage of using this method is that microparticles have been effectively encapsulated during the crosslinking of PEGDMA solution. In experimental applications both degradable poly(lactide-co-glycolide) microparticles (data not shown) and nondegradable polystyrene particles were used to show patterning of controlled-release carriers. Spatial incorporation of controlled-release particles having predesigned release profiles would allow effective temporal patterning of the growth factors necessary for the signaling of progenitor cell differentiation (e.g., growth factor A could be early release and growth factor B could be a late release).

Surfaces of these microfabricated scaffolds must also be functionalized for cell recognition, providing a more biomimetic environment for stem-cell proliferation and behavior. Therefore, ECM components were integrated within scaffolds by covalent conjugation to the scaffolding biomaterial. Fibronectin-derived RGD is a commonly employed amino acid sequence for functionalizing PEG. Scaffolds were functionalized with RGD to be more biomimetic, thereby mediating adhesion to the seeded OP-9 cells. Micrographs show both protein and cellular attachment to the scaffolds that were

modified with RGD. Cells that were seeded onto 100% PEG scaffolds without the presence of RGD did not remain viable.

In addition, one of the key factors in creating hybrid tissue structures is the ability to effectively sequester growth factors and maintain spatial patterning by controlling their diffusion in the scaffold. It was hypothesized that appropriate modifications of the scaffold polymer with ECM components would allow for efficient binding and effective localization of growth factors. To demonstrate spatial patterning as well as localization of specific biofactors, FGF-2 was chosen as a model growth factor. The PEGDMA macromer was premodified with heparan prior to scaffold fabrication in order to regulate activity of the growth factor, FGF-2, and control its diffusion from the prescribed regions. By localizing growth factors into their specific compartments within a single scaffold, molecular signaling for hybrid stem-cell differentiation can be further optimized. Heparan for growth-factor binding was evaluated in both thin-layered and multilayered systems. The immunostaining results show that FGF-2 remained sequestered in a heparan-containing matrix rather than diffusing away, indicating feasibility for successful patterning in a scaffold structure.

Integration of cells within PEG-based scaffolds can be mediated in two different ways: (a) direct cell encapsulation during the crosslinking polymerization, and (b) cell seeding into fabricated scaffolds in which diffusion as well as surface chemistry governs cell distribution. The latter method was chosen for integrating cells within the microfabricated scaffolds, because the predefined channels serve as porosities. It should be noted that the structural material of the scaffold is also a hydrogel that allows for intrinsic diffusivity throughout the scaffold in addition to the presence of channels. It is hypothesized that combining the hydrogel material with a porous macrostructure will allow significantly improved diffusion of oxygen and nutrients to the interior of the scaffold, a major limitation of current scaffolding techniques.

There are, however, some key limitations to this fabrication process in its current form. First, the fabrication process is slow, and if not automated could be tedious, especially for larger scaffold sizes. Thus, cell encapsulation within the hydrogel material, as has been the norm by other researchers using similar materials[14,19,20] is not possible. Instead cells were seeded within the structures. Direct cell encapsulation, however, in combination with laser SL, could prove to be a promising method, because multiple progenitor cells could ultimately be used, mimicking a more complex physiological tissue/organ. It would be helpful to have both options (encapsulation as well as seeding) available. Attempts are being made to increase the speed of the layer-by-layer fabrication process with more advanced optical techniques that would allow both direct encapsulation as well as seeding of cells. Second, staggered layers (to ensure later interconnectivity of pores and channels) have not been achieved. Because in traditional stereolithography such staggering and overhanging structures are quite common and generally achieved with the use of a sacrificial filler material, it is believed that the current technique can be further enhanced using such approaches. Efforts to further enhance the capabilities of this technique to incorporate such features continue. It should be noted that because the walls of the scaffold are hydrogels, lateral diffusion of oxygen and nutrients is possible. Third, the concept of washing off one solution prior to polymerizing another (for spatial patterning) could lead to some cross-contamination between patterns. Although the results indicate that we can successfully pattern several components, it remains to be seen how complex the patterning can be before mixing becomes a problem. However, it is believed that even simple 3D spatial patterns can provide unique insights on cell behavior under complex microenvironments.

In conclusion, a laser-based layer-by-layer photopolymerization process for microfabricating porous polymer scaffolds has been developed. This process allows for precise, predesigned spatial distribution of single or multiple molecules within the scaffold, as well as for the fabrication of predetermined internal architectures. It has also been demonstrated that functionalizing the scaffold material with RGD and heparan ensures efficient cell attachment and allows for spatial sequestration of patterned growth factors (FGF-2). Such microfabricated scaffold structures could provide tools to study progenitor cell populations under patterned, complex microenvironments and ultimately aid in creating predesigned hybrid tissue structures from a single stem-cell population.

The authors thank John Mendenhall and Angela Bardo of the Confocal Facility at The Institute of Cellular and Molecular Biology and Sindura Bandi for technical assistance. This work was supported by grants from the Whitaker Foundation and the National Science Foundation.

REFERENCES

1. Griffith LG. Emerging design principles in biomaterials and scaffolds for tissue engineering. Ann NY Acad Sci 2002;961: 83–95.
2. Orban JM, Marra KG, Hollinger JO. Composition options for tissue-engineered bone. Tissue Eng 2002;8:529–539.
3. Tan JL, Liu W, Nelson CM, Raghavan S, Chen CS. Simple approach to micropattern cells on common culture substrates by tuning substrate wettability. Tissue Eng 2004;10:865–872.
4. Chen CS, Alonso JL, Ostuni E, Whitesides GM, Ingber DE. Cell shape provides global control of focal adhesion assembly. Biochem Biophys Res Commun 2003;307:355–361.
5. Chen CS, Mrksich M, Huang S, Whitesides GM, Ingber DE. Micropatterned surfaces for control of cell shape, position, and function. Biotechnol Prog 1998;14:356–363.
6. Feinberg SE, Hollister SJ, Halloran JW, Chu TM, Krebsbach PH. Image-based biomimetic approach to reconstruction of the temporomandibular joint. Cells Tissues Organs 2001;169:309–321.
7. Hollister SJ, Maddox RD, Taboas JM. Optimal design and fabrication of scaffolds to mimic tissue properties and satisfy biological constraints. Biomaterials 2002;23:4095–4103.
8. Park A, Wu B, Griffith LG. Integration of surface modification and 3D fabrication techniques to prepare patterned poly(L-lactide) substrates allowing regionally selective cell adhesion. J Biomater Sci Polym Ed 1998;9:89–110.
9. Sachlos E, Czernuszka JT. Making tissue engineering scaffolds work. Review: the application of solid freeform fabrication

technology to the production of tissue engineering scaffolds. Eur Cell Mater 2003;5:29–39.
10. Richardson TP, Peters MC, Ennett AB, Mooney DJ. Polymeric system for dual growth factor delivery. Nat Biotechnol 2001; 19:1029–1034.
11. Elisseeff J, McIntosh W, Anseth K, Riley S, Ragan P, Langer R. Photoencapsulation of chondrocytes in poly(ethylene oxide)-based semi-interpenetrating networks. J Biomed Mater Res 2000;51:164–171.
12. Elisseeff J, McIntosh W, Fu K, Blunk BT, Langer R. Controlled-release of IGF-I and TGF-beta1 in a photopolymerizing hydrogel for cartilage tissue engineering. J Orthop Res 2001; 19:1098–1104.
13. Bryant SJ, Anseth KS. Hydrogel properties influence ECM production by chondrocytes photoencapsulated in poly(ethylene glycol) hydrogels. J Biomed Mater Res 2002;59:63–72.
14. Burdick JA, Anseth KS. Photoencapsulation of osteoblasts in injectable RGD-modified PEG hydrogels for bone tissue engineering. Biomaterials 2002;23:4315–4323.
15. Hedberg EL, Tang A, Crowther RS, Carney DH, Mikos AG. Controlled release of an osteogenic peptide from injectable biodegradable polymeric composites. J Control Release 2002; 84:137–150.
16. Burkoth AK, Anseth KS. A review of photocrosslinked polyanhydrides: *in situ* forming degradable networks. Biomaterials 2000;21:2395–2404.
17. Anseth KS, Shastri VR, Langer R. Photopolymerizable degradable polyanhydrides with osteocompatibility. Nat Biotechnol 1999;17:156–159.
18. Halstenberg S, Panitch A, Rizzi S, Hall H, Hubbell JA. Biologically engineered protein-graft-poly(ethylene glycol) hydrogels: a cell adhesive and plasmin-degradable biosynthetic material for tissue repair. Biomacromolecules 2002;3:710–723.
19. Nuttelman CR, Tripodi MC, Anseth KS. *In vitro* osteogenic differentiation of human mesenchymal stem cells photoencapsulated in PEG hydrogels. J Biomed Mater Res A 2004;68:773–782.
20. Williams CG, Kim TK, Taboas A, Malik A, Manson P, Elisseeff J. *In vitro* chondrogenesis of bone marrow–derived mesenchymal stem cells in a photopolymerizing hydrogel. Tissue Eng 2003;9:679–688.
21. Alhadlaq A et al., Adult stem cell driven genesis of human-shaped articular condyle. Ann Biomed Eng 2004;32:911–923.
22. Kim TK, Sharma B, Williams CG, Ruffner MA, Malik A, McFarland EG, Elisseeff JH. Experimental model for cartilage tissue engineering to regenerate the zonal organization of articular cartilage. Osteoarthritis Cartilage 2003;11:653–664.
23. Taipale J, Keski-Oja J. Growth factors in the extracellular matrix. FASEB J 1997;11:51–59.
24. Allen BL, Filla MS, Rapraeger AC. Role of heparan sulfate as a tissue-specific regulator of FGF-4 and FGF receptor recognition. J Cell Biol 2001;155:845–858.
25. Pye DA, Vives RR, Hyde P, Gallagher JT. Regulation of FGF-1 mitogenic activity by heparan sulfate oligosaccharides is dependent on specific structural features: differential requirements for the modulation of FGF-1 and FGF-2. Glycobiology 2000;10: 1183–1192.
26. Richard C, Roghani M, Moscatelli D. Fibroblast growth factor (FGF)-2 mediates cell attachment through interactions with two FGF receptor-1 isoforms and extracellular matrix or cell-associated heparan sulfate proteoglycans. Biochem Biophys Res Commun 2000;276:399–405.
27. Lin X, Buff EM, Perrimon N, Michelson AM. Heparan sulfate proteoglycans are essential for FGF receptor signaling during Drosophila embryonic development. Development 1999;126: 3715–3723.
28. Rahmoune H, Chen HL, Gallagher JT, Rudland PS, Fernig DG. Interaction of heparan sulfate from mammary cells with acidic fibroblast growth factor (FGF) and basic FGF. Regulation of the activity of basic FGF by high and low affinity binding sites in heparan sulfate. J Biol Chem 1998;273:7303–7310.
29. Quarto N, Amalric F. Heparan sulfate proteoglycans as transducers of FGF-2 signalling. J Cell Sci 1994;107:3201–3212.
30. Gleizes PE, Noaillac-Depeyre J, Amalric F, Gas N. Basic fibroblast growth factor (FGF-2) internalization through the heparan sulfate proteoglycans-mediated pathway: an ultrastructural approach. Eur J Cell Biol 1995;66:47–59.
31. Bryant SJ, Nuttelman CR, Anseth KS. Cytocompatibility of UV and visible light photoinitiating systems on cultured NIH/3T3 fibroblasts *in vitro*. J Biomater Sci Polym Ed 2000;11:439–457.
32. Koh WG, Revzin A, Pishko MV. Poly(ethylene glycol) hydrogel microstructures encapsulating living cells. Langmuir 2002; 18:2459–2462.
33. Davis KA, Anseth KS. Controlled release from crosslinked degradable networks. Crit Rev Ther Drug Carrier Syst 2002;19: 385–423.
34. Metters AT, Anseth KS, Bowman CN. Fundamental studies of biodegradable hydrogels as cartilage replacement materials. Biomed Sci Instrum 1999;35:33–38.
35. Taboas JM, Maddox RD, Krebsbach PH, Hollister SJ. Indirect solid free form fabrication of local and global porous, biomimetic and composite 3D polymer-ceramic scaffolds. Biomaterials 2003;24:181–194.
36. Lin CY, Kikuchi N, Hollister SJ. A novel method for biomaterial scaffold internal architecture design to match bone elastic properties with desired porosity. J Biomech 2004;37:623–636.
37. Hollister SJ, Levy RA, Chu TM, Halloran JW, Feinberg SE. An image-based approach for designing and manufacturing craniofacial scaffolds. Int J Oral Maxillofac Surg 2000;29:67–71.